Parameterization of subgrid-scale stress by the velocity gradient tensor

By T. S. Lund AND E. A. Novikov[1]

1. Motivation and objectives

In large eddy simulation (LES), the large scale motions are directly computed and the effects of the small scales are modeled. The term to be modeled is the subgrid-scale stress tensor,

$$\tau_{ij} = \overline{u_i u_j} - \bar{u}_i \bar{u}_j, \tag{1}$$

which arises when the Navier-Stokes equations are spatially filtered (denoted by overbar) to remove the small scale information. Most large eddy simulations make use of the Smagorinsky (1963) eddy-viscosity model,

$$\tau_{ij} - \frac{1}{3}\tau_{kk}\delta_{ij} = -2(C\Delta^2|\bar{S}|)\bar{S}_{ij}, \tag{2}$$

where C is a non-dimensional constant, Δ is the grid spacing, and $\bar{S}_{ij}$ is the resolved strain-rate.

Although the Smagorinsky model has been in use for nearly thirty years, for roughly half that period it has been known that the model provides only a crude estimate for the stresses. This fact was first demonstrated by Clark *et al.* (1979), where direct numerical simulation (DNS) data for homogeneous isotropic turbulence was used to evaluate model predictions. Clark *et al.* found a correlation coefficient of approximately 0.2 when comparing predictions of the Smagorinsky model with the exact stresses. McMillan *et al* (1979) found that the correlation coefficient was even lower in homogeneous shear flow, being close to 0.1. Later, Piomelli *et al.* (1988) found similar results in turbulent channel flow.

When contemplating these extremely low correlations, it may seem striking that the Smagorinsky model is successful when used in a large eddy simulation. The reason for the seemingly unwarranted accuracy is that, by construction, the Smagorinsky model insures a net drain of energy from the large scales to the subgrid-scale motions. This is the primary objective of the subgrid-scale model, and as long as this requirement is met, reasonable results are evidently obtained. On the other hand, the Smagorinsky model provides poor predictions of the individual elements of the stress tensor. It is natural to expect that superior results could be obtained with a model that predicts the stress tensor more accurately. The aim of this work is to seek out potentially more accurate models.

The Smagorinsky model is based on a molecular transport analogy where the stress is proportional to the rate of strain. The molecular analogy is a rather crude

1 Permanent address: Institute for Nonlinear Science, University of California, San Diego

model for turbulent transport, however, and it may be expected that a more accurate model for the subgrid-scale stress could be obtained if additional information were included. An obvious quantity to consider is the vorticity (or equivalently the rotation rate tensor). While molecular transport is unaffected by rotation, there is no reason to exclude rotation from a model for turbulent transport. Indeed, vortex stretching is believed to be the dominant mechanism by which turbulence transfers energy from large to smaller scales (Tennekes & Lumley 1971).

The objective of this work is to construct and evaluate subgrid-scale models that depend on both the strain rate and the vorticity. This will be accomplished by first assuming that the subgrid-scale stress is a function of the strain and rotation rate tensors. Extensions of the Caley-Hamilton theorem can then be used to write the assumed functional dependence explicitly in the form of a tensor polynomial involving products of the strain and rotation rates. Finally, use of this explicit expression as a subgrid-scale model will be evaluated using direct numerical simulation data for homogeneous, isotropic turbulence.

2. Accomplishments

2.1 Subgrid-scale stress as a tensor function of strain and rotation rates

It is assumed that the residual stress may be written as a function of the strain and rotation rate tensors, as well as the unit isotropic tensor, *viz.*

$$\tau_{ij} = f(S_{ij}, R_{ij}, \delta_{ij}), \tag{3}$$

where the strain and rotation rate tensors are defined as

$$S_{ij} = \frac{1}{2}\left(\frac{\partial \bar{u}_i}{\partial x_j} + \frac{\partial \bar{u}_j}{\partial x_i}\right), \tag{4a}$$

$$R_{ij} = \frac{1}{2}\left(\frac{\partial \bar{u}_i}{\partial x_j} - \frac{\partial \bar{u}_j}{\partial x_i}\right), \tag{4b}$$

and where $\bar{u}_i$ is the resolved velocity. Note that S and R are the symmetric and antisymmetric parts of the velocity gradient tensor. Thus Eq. (3) can be alternatively interpreted as a relationship between the subgrid-scale stress and the velocity gradient tensor.

For simplicity in the following development, a matrix notation is introduced. Let $\boldsymbol{\tau}$, $\mathbf{S}$, $\mathbf{R}$, and $\mathbf{I}$ be the matrices associated with the corresponding tensor quantities ($\mathbf{I}$ is the identity matrix associated with δ_{ij}). Tensor contractions correspond to matrix multiplications in the following way:

$$\mathbf{SR} = S_{ik}R_{kj}, \qquad \mathbf{R}^2 = R_{ik}R_{kj}, \quad \text{etc.}, \tag{5a}$$

$$\mathrm{tr}\,(\mathbf{SR}^2) = S_{ij}R_{jk}R_{ki}, \quad \text{etc.} \tag{5b}$$

The most general expression for Eq. (3) is an infinite tensor polynominal containing terms of the form $\mathbf{S}^{\alpha_1}\mathbf{R}^{\beta_1}\mathbf{S}^{\alpha_2}\mathbf{R}^{\beta_2}\ldots$, where α_i and β_i are positive integers.

Each term in the series is multiplied by a coefficient that may be a function of the simultaneous invariants of **S** and **R** (discussed below). The Caley-Hamilton theorem of matrix algebra (see Pipes & Hovanessian 1969) states that terms in the polynomial beyond a certain order are redundant, and thus the infinite polynomial is equivalent to one involving a finite number of terms. Spencer and Rivlin (1959) have determined the surviving terms when one tensor is expressed in terms of two others, as done here. Since the subgrid-scale stress is symmetric, only the symmetric tensors in this list need to be considered. When the Results of Spencer and Rivlin are applied to the present situation and the results properly symmetrized, the following tensors and associated invariants arise:

$$\begin{aligned}
\mathbf{m}_1 &= \mathbf{S}, & \mathbf{m}_2 &= \mathbf{S}^2, \\
\mathbf{m}_3 &= \mathbf{R}^2, & \mathbf{m}_4 &= \mathbf{SR} - \mathbf{RS}, \\
\mathbf{m}_5 &= \mathbf{S}^2\mathbf{R} - \mathbf{RS}^2, & \mathbf{m}_6 &= \mathbf{I}, \\
\mathbf{m}_7 &= \mathbf{SR}^2 + \mathbf{R}^2\mathbf{S}, & \mathbf{m}_8 &= \mathbf{RSR}^2 - \mathbf{R}^2\mathbf{SR}, \\
\mathbf{m}_9 &= \mathbf{SRS}^2 - \mathbf{S}^2\mathbf{RS}, & \mathbf{m}_{10} &= \mathbf{S}^2\mathbf{R}^2 + \mathbf{R}^2\mathbf{S}^2, \\
\mathbf{m}_{11} &= \mathbf{RS}^2\mathbf{R}^2 - \mathbf{R}^2\mathbf{S}^2\mathbf{R}, &&
\end{aligned} \tag{6}$$

$$\begin{aligned}
I_1 &= \mathrm{tr}\left(\mathbf{S}^2\right), & I_2 &= \mathrm{tr}\left(\mathbf{R}^2\right), \\
I_3 &= \mathrm{tr}\left(\mathbf{S}^3\right), & I_4 &= \mathrm{tr}\left(\mathbf{SR}^2\right), \\
I_5 &= \mathrm{tr}\left(\mathbf{S}^2\mathbf{R}^2\right), & I_6 &= \mathrm{tr}\left(\mathbf{S}^2\mathbf{R}^2\mathbf{SR}\right).
\end{aligned} \tag{7}$$

These results were presented earlier by Pope (1975) in connection with models for the Reynolds averaged Navier-Stokes equations. The invariant I_6, however, was not included in Pope's analysis. This invariant is anomalous in the sense that it is related to the other 5 but with an ambiguity in sign. The relationship is

$$\begin{aligned}
I_6 = \pm[\, &(4\hat{I}_1^3 + \hat{I}_3^2)\hat{I}_2^3 - \hat{I}_3 I_4^3 - I_5^3 + 4\hat{I}_1(\hat{I}_3 I_4 - 2\hat{I}_1 I_5)\hat{I}_2^2 + \\
&\hat{I}_1(I_5 - \hat{I}_1\hat{I}_2)I_4^2 + 5\hat{I}_1\hat{I}_2 I_5^2 - 3\hat{I}_2\hat{I}_3 I_4 I_5\,]^{1/2},
\end{aligned}$$

where $\hat{I}_1 = I_1/2$, $\hat{I}_2 = I_2/2$, and $\hat{I}_3 = I_3/3$. The sign ambiguity can be resolved by replacing the $\pm$ above by the multiplicative factor $\mathrm{sign}(\tilde{w}_1\tilde{w}_2\tilde{w}_3)$, where $\tilde{w}_1$, $\tilde{w}_2$, and $\tilde{w}_3$ are the vorticity components expressed in the principal coordinate system of the strain rate tensor. (The function $\mathrm{sign}(x)$ returns either -1 for $x < 0$ or 1 for $x > 0$.) Since resolution of the sign ambiguity requires information that is not contained in the invariants I_1, I_2, ... I_5, the invariant I_6 may be considered to be independent of the other 5. For this reason, we shall include I_6 in the subsequent analysis.

The set of tensors displayed in Eq. (6) are complete in the sense that any symmetric polynomial involving products of **S** and **R** can be written as a linear combination of the 11 tensors, with the scalar multipliers expressed as polynomials of the 6 invariants. The tensors are also independent in the sense that none of the 11 tensors

may be written as a linear combination of the other 10 if the scalar multipliers are restricted to be polynomials of the 6 invariants. If this restriction is relaxed slightly so that the scalar multipliers may be *ratios* of polynomials of the invariants, then under the conditions discussed below only 6 of the above 11 tensors are independent (see Rivlin and Ericksen (1955) for more details). To see this, consider expressing one of the 11 tensors as a linear combination of 6 others:

$$\mathbf{m}_k = C_i \mathbf{m}_i; \qquad i = 1, 2, \ldots 6, \quad k > 6, \tag{8}$$

where the tensors are ordered in any desired way, not necessarily as in Eq. (6). Due to symmetry, each of the tensors $\mathbf{m}_i$ have only 6 unique elements. Thus Eq. (8) represents 6 algebraic equations for the 6 unknown coefficients C_i. The solution can be written as

$$C_i = [\mathrm{tr}\,(\mathbf{m}_i \mathbf{m}_j)]^{-1} \mathrm{tr}\,(\mathbf{m}_k \mathbf{m}_j)\,. \tag{9}$$

A unique solution will exist provided the above matrix of traces is non-singular, that is

$$\det[\mathrm{tr}\,(\mathbf{m}_i \mathbf{m}_j)] \neq 0. \tag{10}$$

Note that if Eq. (9) is solved by Cramer's rule, the C_i will be expressed as a ratios of polynomials of the invariants listed in Eq. (7).

Equation (10) can be violated under two conditions: when $\mathbf{S}$ has a repeated eigenvalue, or when two components of the vorticity, expressed in the principal coordinates of $\mathbf{S}$, vanish. The first condition corresponds to an axisymmetric state of strain. The second corresponds to a situation where the rotation is confined to a single axis, and this axis is aligned with one of the principal directions of the strain rate. Although either of these conditions could be realized in a turbulent field, the probability of exactly satisfying either of them is rather remote. Indeed, when the tensor expansion was evaluated using direct numerical simulation data as described in the following section, the conditions for lack of independence were never satisfied exactly, even for 128^3 realizations.

Assuming that Eq. (10) is satisfied, only the first 6 terms in Eq. (6) need to be considered. For incompressible flows, it is customary to model only the deviatoric part of τ and combine the isotropic part with the pressure. We shall follow the precedent here and subtract the trace from each of the first 6 tensors in Eq. (6). The 6th term vanishes when this is done, leaving only the first 5 as a basis. This is consistent with the fact that a trace-free symmetric tensor has only 5 unique elements. This result could have been obtained equivalently by subtracting the trace from each of the 11 tensors at the outset and then showing that any tensor in the list can be written as a linear combination of the first 5. In any event, the stress can be written as

$$\begin{aligned} \tau^* = & C_1 \Delta^2 |\mathbf{S}| \mathbf{S} + C_2 \Delta^2 (\mathbf{S}^2)^* + C_3 \Delta^2 (\mathbf{R}^2)^* + \\ & C_4 \Delta^2 (\mathbf{SR} - \mathbf{RS}) + C_5 \Delta^2 \frac{1}{|\mathbf{S}|} (\mathbf{S}^2 \mathbf{R} - \mathbf{R}\mathbf{S}^2), \end{aligned} \tag{11}$$

where Δ is the grid spacing, $|\mathbf{S}| = \sqrt{\mathrm{tr}(\mathbf{S}^2)}$, and $()^*$ indicates the trace-free part. Use of the strain rate magnitude as a scaling factor was chosen somewhat arbitrarily. In theory, this is not an issue since the C_i can depend on all of the invariants in Eq. (7) and the correct scaling will be obtained if the C_i are written as functions of the invariants. In practice, it is difficult to find the dependence of the C_i on the invariants, and thus the choice of the scaling becomes relevant. Several alternate scalings were tested and the results appeared to be quite insensitive to the particular choice.

Since the expansion coefficients C_i are non-dimensional, they can depend only on non-dimensional groupings of the invariants listed in Eq. (7). These are taken to be

$$s_1 = \frac{\mathrm{tr}(\mathbf{S}^3)}{\mathrm{tr}(\mathbf{S}^2)^{3/2}}, \tag{12a}$$

$$s_2 = \frac{\mathrm{tr}(\mathbf{R}^2)}{\mathrm{tr}(\mathbf{S}^2)}, \tag{12b}$$

$$s_3 = \frac{\mathrm{tr}(\mathbf{S}\mathbf{R}^2)}{\mathrm{tr}(\mathbf{S}^2)^{1/2}\mathrm{tr}(\mathbf{R}^2)}, \tag{12c}$$

$$s_4 = \frac{\mathrm{tr}(\mathbf{S}^2\mathbf{R}^2)}{\mathrm{tr}(\mathbf{S}^2)\,\mathrm{tr}(\mathbf{R}^2)}. \tag{12d}$$

$$s_5 = \frac{\mathrm{tr}(\mathbf{S}^2\mathbf{R}^2\mathbf{S}\mathbf{R})}{[\mathrm{tr}(\mathbf{S}^2)\,\mathrm{tr}(\mathbf{R}^2)](3/2)}. \tag{12e}$$

2.2 Evaluation of the proposed model

Equation (11) is an exact result that will hold as long a the basic assumption that the stress is expressible solely as a function of the strain and rotation rates is correct(i.e. Eq. (3)). Thus under this assumption, the stress τ can be represented exactly in terms of the strain and rotation rate tensors, provided the coefficients C_i are known functions of the invariants listed in Eq. (12). The functional form of the dependence on the invariants is unknown, however, and can not be determined easily. If the assumption that the stress is expressible solely as a function of the strain and rotation rates is not correct, then the coefficients will be functions of the unknown quantities on which the stress really depends. In either case, it can be anticipated that it will be difficult to predict the spatial variation of the expansion coefficients.

In the context of modeling, the expansion coefficients would most likely be assigned constant values that reflect an overall "best-fit" for all points in the field. If the true coefficient values do not vary greatly in space, then taking them to be constant will be a reasonable approximation and a good representation of the stresses can be expected. On the other hand, if the coefficients vary greatly in space, then taking them to be constant would be a poor approximation and the model would be of little value. Thus, in practical terms, the utility of this approach depends on the

degree to which the expansion coefficients vary or, alternately, how well Eq. (11) is satisfied for fixed coefficients.

The issue of coefficient variability was investigated through the use of direct numerical simulation (DNS) data of homogeneous, isotropic turbulence. By filtering the DNS field with a spectral cutoff filter, the subgrid-scale stress, as well as the "resolved" strain and rotation rates were computed exactly. The accuracy of Eq. (11) was then measured in two alternate ways: (1) by determining the expansion coefficients exactly at each grid point and then measuring their spatial variation and (2) by measuring the degree to which Eq. (11) was satisfied when the coefficients were assigned constant values.

The homogeneous, isotropic data was generated with a pseudo-spectral code (Rogallo, (1981) on a 128^3 mesh. The energy spectrum was initialized according to

$$E(k) = \frac{1}{32}\left(\frac{k}{2}\right)^4 \exp\left(-\frac{k}{2}\right). \tag{13}$$

This spectrum has its energy peak at wavenumber 8. The initial phases were chosen randomly, but in such a way that the divergence-free condition was satisfied (see Rogallo, (1981) for more details on the initial conditions). The flow was allowed to evolve freely for 2.9 small scale eddy turnover times, $\frac{\lambda}{u'}$ where λ is the Taylor microscale and u' is the rms turbulence intensity, both based on the final field. Over this period of time, the total turbulent kinetic energy decayed by 33%. The final Taylor microscale Reynolds number ($u'\lambda/\nu$) was 45.3, and the velocity derivative skewness was -0.32. The final energy spectrum, scaled in Kolmogorov units, is plotted in Figure 1.

Also shown in Figure 1 are the experimental data of Comte-Bellot and Corrsin (1971). The simulation results fit well with the experimental data. The tail-up in the simulated spectrum at high wavenumbers is a characteristic of spectral methods and is more pronounced when the dissipation range is not fully resolved, as in this case. It is generally felt (Rogallo, private communication) that the tail-up at high wavenumber will not adversely affect the data in the central portion of the spectrum used here.

Following the procedure of Clark *et al.*(1975), a synthetic LES velocity field was generated from the DNS data by filtering out the small scale motions. The filtering was achieved via spherical truncation in wave space where three quarters of the active high frequency modes were removed. The LES field thus corresponded to an isotropic simulation performed on a $128/4 = 32$ cubed mesh. Denoting the filtering operation with an overbar, the subgrid-scale stress was determined by performing the operations in the de-aliased definition commonly used in spectral calculations,

$$\tau_{ij} = \overline{u_i u_j} - \overline{u_i}\,\overline{u_j}. \tag{14}$$

The large scale strain and rotation rate tensors defined in Eq. (4) were determined by applying spectral derivative operators to the LES velocity field.

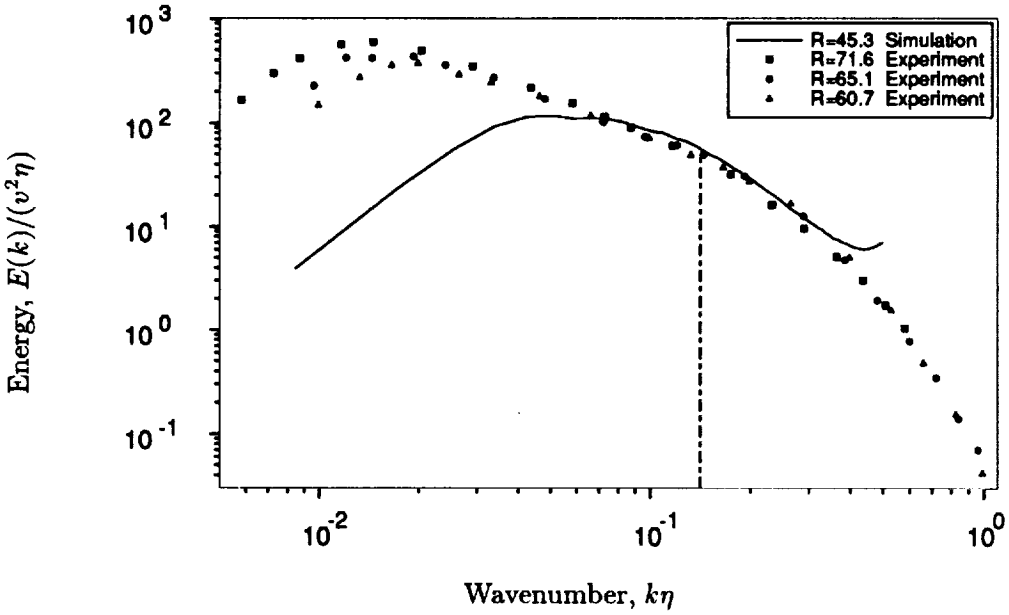

FIGURE 1. Energy spectrum from the DNS data base. The experimental data are taken from Comte-Bellot and Corrsin (1971). The vertical line corresponds to the scale at which the velocity field was filtered to generate the synthetic LES field.

2.3 Analysis for variable coefficients

With the subgrid-scale stress and the large scale strain and rotation rate tensors known, the expansion coefficients in Eq. (11) could be determined at each point in the field. This was done using a least-squares fitting procedure so that solutions could be obtained when less than all five of the tensors on the right hand side of Eq. (11) were used. To derive the least-squares expression, consider the error in satisfying Eq. (11) when an arbitrary number of tensors are used:

$$\mathbf{E} = C_i \mathbf{m}_i - \boldsymbol{\tau}, \tag{15}$$

where $\mathbf{m}_i$ are the model tensors on the right hand side of Eq. (11), and $i = 1, 2, ...n$; $1 \leq n \leq 5$. The square of the error will be minimized with respect to the C_i if the following condition is enforced

$$\frac{\partial}{\partial C_i} \mathrm{tr}\left(\mathbf{E}^2\right) = 0. \tag{16}$$

This condition leads to the following algebraic system for the coefficients:

$$C_i = [\mathrm{tr}\left(\mathbf{m}_i \mathbf{m}_j\right)]^{-1} \mathrm{tr}\left(\mathbf{m}_j \boldsymbol{\tau}\right). \tag{17}$$

If less than 5 model tensors are used, the subgrid-scale stress can not be represented exactly by Eq. (11). The following quantities are global measures of the error in this case:

$$\eta = \frac{< \mathrm{tr}\left(\boldsymbol{\tau}\mathbf{M}\right) >}{\sqrt{< \mathrm{tr}\left(\boldsymbol{\tau}^2\right) >< \mathrm{tr}\left(\mathbf{M}^2\right) >}}, \tag{18}$$

$$e_\tau = \sqrt{\frac{< \mathrm{tr}\left((\boldsymbol{\tau} - \mathbf{M})^2\right) >}{< \mathrm{tr}\,(\boldsymbol{\tau}^2) >}}, \tag{19}$$

where $\mathbf{M} = C_i \mathbf{m}_i$ is the composite model tensor and $<>$ denotes a volume average. The quantity η is the correlation coefficient between the exact and modeled stress, while e_τ is the rms error in the subgrid-scale stress. It is easy to show that η and e_τ are related via $e_\tau = \sqrt{1 - \eta^2}$. The variability of the coefficients themselves was measured in terms of the ratio of rms to mean value:

$$C_{rms} = \frac{\sqrt{< C^2 > - < C >^2}}{< C >}. \tag{20}$$

2.3.1 Results

As a first step, each of the 5 terms in Eq. (11) was considered separately. Measures of the error as well as coefficient variability were recorded for each term. Next, the 10 possible pairs of terms in Eq. (11) were investigated. The 10 possible triplets, the 5 possible quadruplets, and finally all 5 terms together were tested. For each of the groupings, the combinations that resulted in the highest as well as the lowest correlation coefficients were selected for further study. Figure 2 shows these correlation coefficients as a function of the number of terms in the group. As expected, the correlation coefficient rises as more terms are added and is unity if all five terms are present. The differences between the best and worst correlation coefficients are rather slight, indicating that none of the terms are neither far superior nor far inferior to the rest. The terms forming the best and worst subsets are listed in Table 1.

Number of terms	Best combination	Worst combination
1	1	3
2	1, 4	2, 3
3	1, 4, 5	3, 4, 5
4	1, 2, 4, 5	2, 3, 4, 5
5	1, 2, 3, 4, 5	1, 2, 3, 4, 5

TABLE 1. Best and worst subsets of the model terms in Eq. (11) - variable coefficients.

Although the differences between correlation coefficients obtained with the best and worst groupings are slight, there are some consistent trends if the terms are ranked by their relative importance. The best single term is term 1, which corresponds to the Smagorinsky model. This term is present in each of the optimal

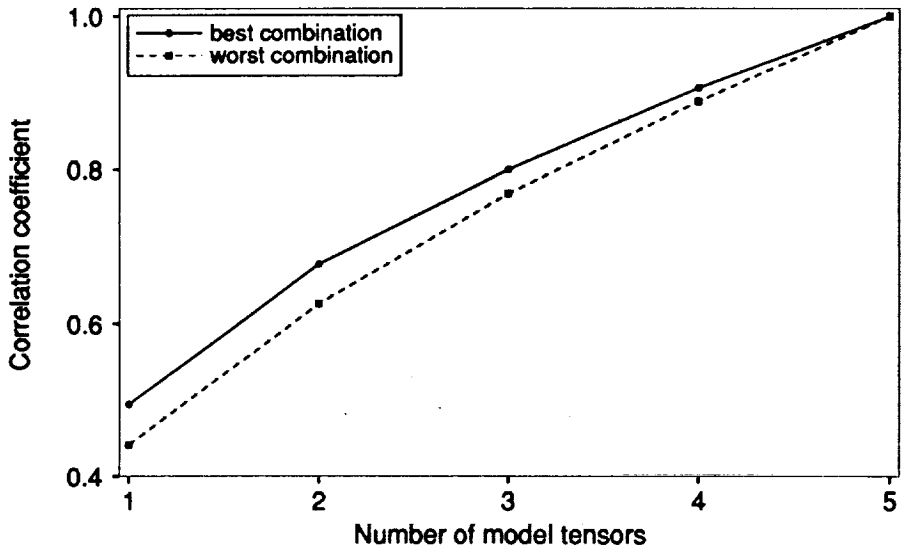

FIGURE 2. Correlation coefficients for the best and worst subsets of the terms in Eq. (11) - variable coefficients.

groupings. The worst single term is the rotation rate squared (term 3). This term is also the last one to enter in the optimal groupings. Most of the intermediate terms follow the general trend that if they enter the optimal groupings when n terms are present, then they enter the worst grouping when $5 - n$ terms are used.

Although ranking the various combinations of terms by their correlation coefficients is interesting, the more important issue is spatial variability of the corresponding expansion coefficients. The ratio of the coefficient rms to the coefficient mean for the optimal groupings of terms is shown in Figure 3. It is clear that a substantial variation in each coefficient is required to achieve the least-squares fit. If only one term is included, the coefficient variation is roughly three times the mean. As more terms are included, the variation rapidly increases. When all five terms are included, the coefficient variation is enormous, ranging from roughly 10 times the mean for C_1 to over 500 times the mean for C_3.

The rather large coefficient variation could in part be due to the the neglected dependence on the invariants listed in Eq. (12). It is conceivable that if this dependence were taken into account, the coefficient variability could be reduced. This issue is explored in the following section.

2.4 Dependence on the invariants

Each of the expansion coefficients in Eq. (11) can, in principal, depend of the five invariants listed in Eq. (12). Determining such a dependence in a five parameter space is a difficult task, however. One way to do this would be to divide the range of each invariant into m intervals, thereby partitioning the parameter space into m^5

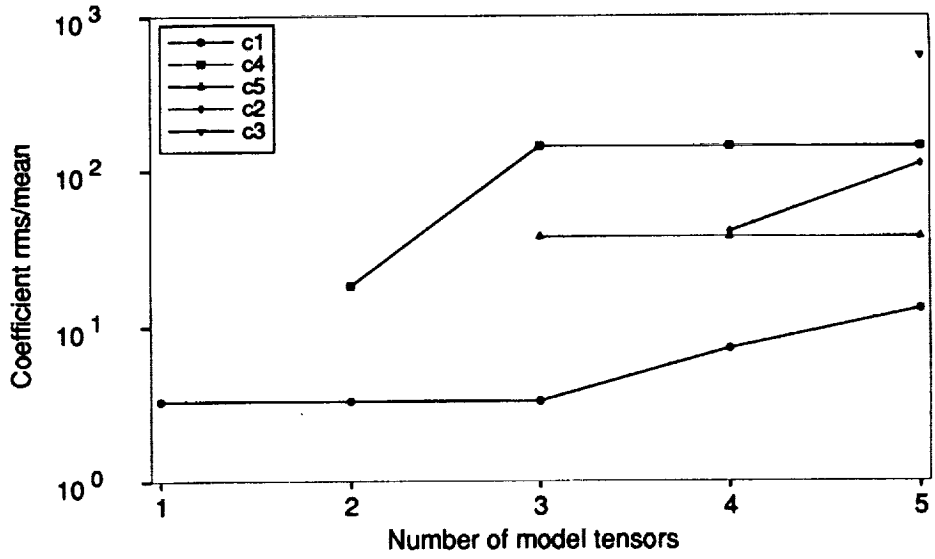

FIGURE 3. Coefficient variability for optimal subsets of the terms in Eq. (11).

hypercubes. Using the DNS data, the coefficients could then be sorted according to their associated invariant values and the resulting sample averaged over each hypercube. Unfortunately, this procedure requires an enormous amount of data if reliable statistics are to be obtained. As an illustration, consider the following example. If 16 intervals are chosen for the discretization and a 128^3 DNS data base is used, there will be on the average only $128^3/16^5 = 2$ samples within each hypercube. This sample is clearly too small to provide meaningful statistics. Furthermore, it may be anticipated that many of the cubes will contain no data at all. If a larger data base or more realizations are used and if the number of intervals is reduced, it may be possible to obtain reliable statistics. If this were done, the difficult task of fitting the statistical data with some sort of multidimensional function would still remain.

In view of these difficulties, two alternate approaches have been adopted here. In the first, the number of invariants was reduced to one by assuming that the stress depended only on the strain rate. The local smoothing procedure described above was used in this case since the sample size was large and the resulting one-dimensional function could be easily curve fit. In the second approach, the full problem was considered and a sophisticated regression algorithm was used to find any dependence as well as its associated functional form.

2.4.1 Dependence on a single invariant

The question of dependence on the invariants can be answered completely if it is first assumed that the stress depends only on the strain rate. In this case, the Caley-Hamilton theorem states that the stress can be explicitly written as a linear

combination of $\mathbf{S}$, $\mathbf{S}^2$, and $\mathbf{I}$ (all higher powers of $\mathbf{S}$ are related to these three terms). If only the deviatoric part of $\boldsymbol{\tau}$ is to be modeled, then only $\mathbf{S}$ and $(\mathbf{S}^2)^*$ are required. Thus Eq. (11) reduces to first two terms in this case. The corresponding coefficients, C_1 and C_2, could depend at most on the invariant s_1 listed in Eq. (12).

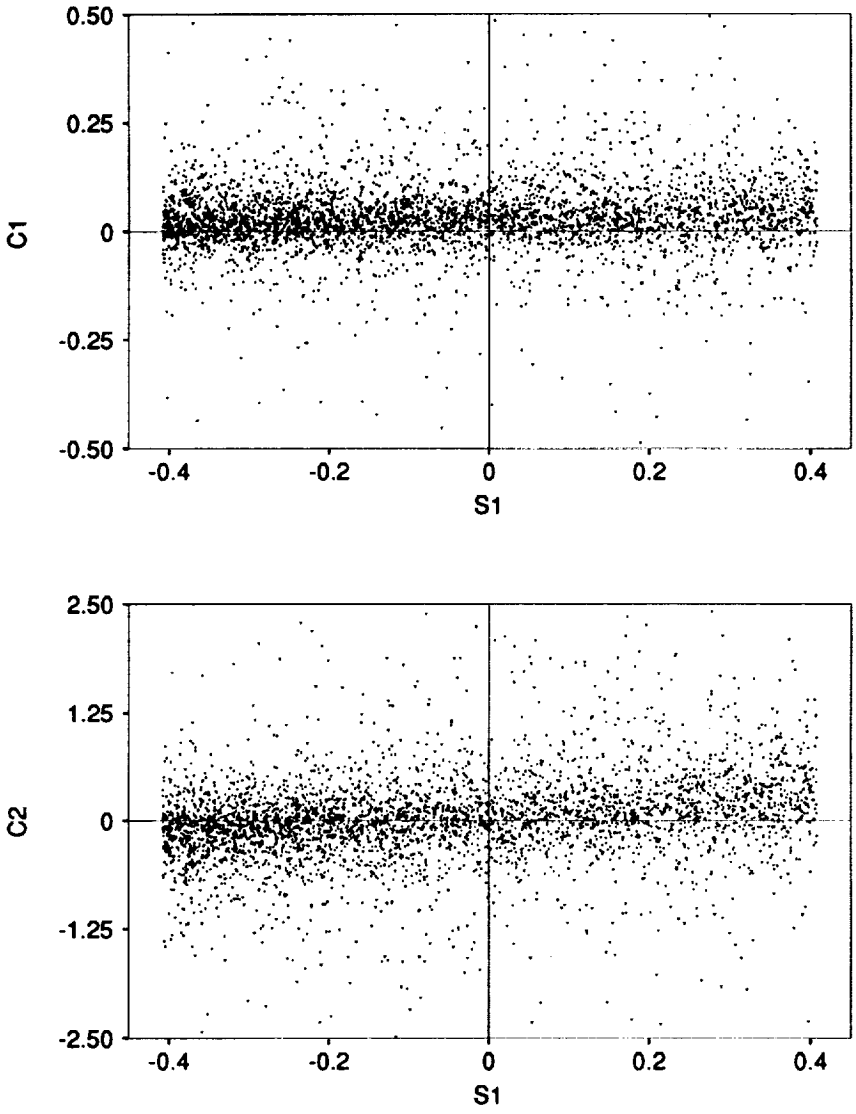

FIGURE 4. Scatter plot of model coefficients versus the invariant s_1. Only every 8^{th} data point in each direction is plotted.

This abbreviated model was tested as in section 2.3, with the coefficients determined locally. The resulting coefficients are plotted as a function of the associated

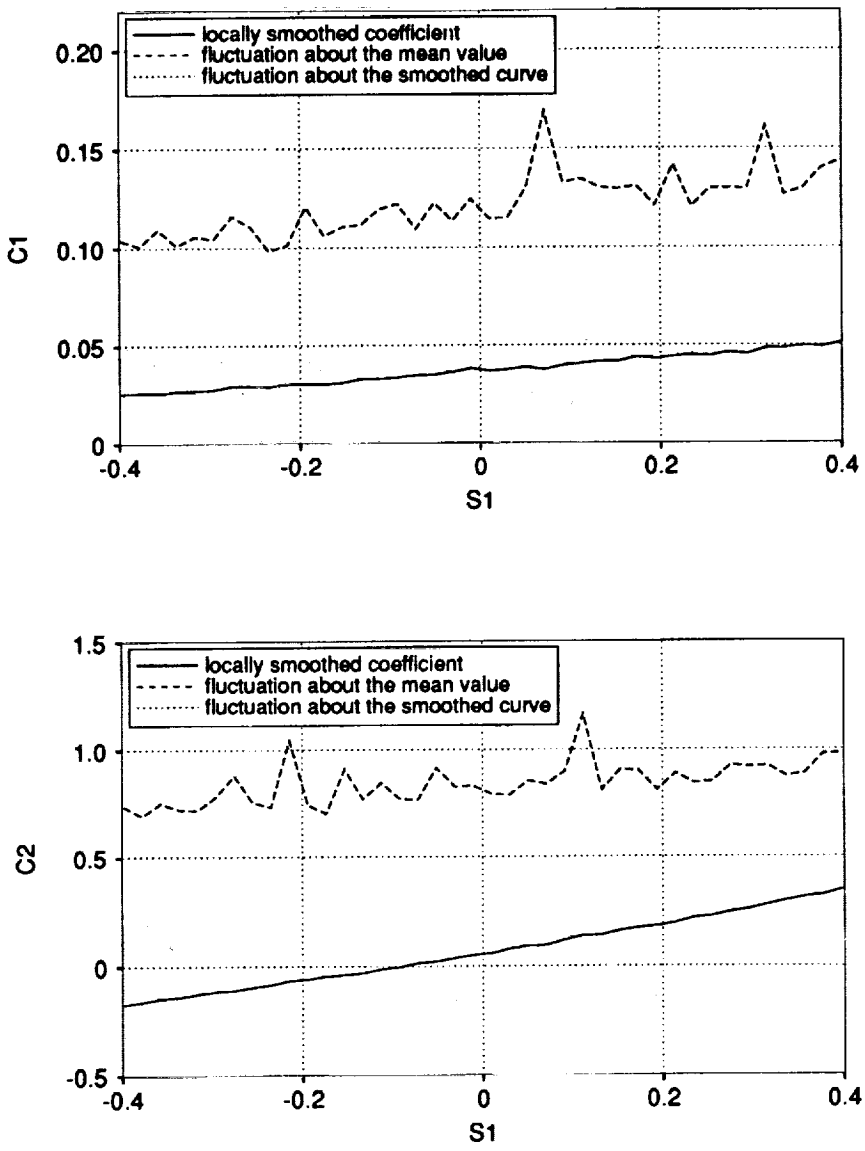

FIGURE 5. Model coefficient conditionally averaged on invariant s_1.

invariant value in Figure 4. There does not seem to be any strong dependence on the invariant in either case. If the raw data are averaged over narrow intervals in s_1, however, a weak trend emerges. The results of such an averaging are shown in Figure 5. It appears that both C_1 and C_2 depend linearly on the invariant s_1. Also shown in Figure 5 is the rms fluctuation of the data about the smoothed curve as

well as the rms fluctuation about the coefficient mean value. There is no visible reduction in the fluctuation level if the dependence on the invariant is accounted for. Thus while a clear dependence on the invariant was found, it accounts for vary little of the coefficient variation.

2.4.2 Dependence on all five invariants: Projection pursuit regression

Although the local smoothing procedure described in Section 2.4 does not seem suitable for this problem, there are other numerical methods that can perform multi-variable regression, even for a moderate sample size. Perhaps the best of these methods is the projection pursuit regression algorithm developed by Friedman and Stuetzle in 1981. The algorithm consists of a numerical optimization routine that finds one dimensional projections of the original independent variables for which the best correlations with the dependent variable can be obtained. The dependent variable is then written as a sum of empirically determined functions of these projections. The method is quite robust and has been able to determine nonlinear relationships within a 5 parameter space using only 213 realizations (see Friedman and Stuetzle (1982) for more details and examples). The method has also been used by Meneveau *et al.* (1992) to search DNS data for improved subgrid-scale model parameterizations.

The projection pursuit algorithm was used to search for coefficient dependence on the five invariants. The DNS data was used to determine the five expansion coefficients and five invariants at each point in the field. This data was then input to the projection pursuit algorithm and each coefficient was analyzed independently. For each coefficient, the numerical optimization routine was able to find projections for which the variance was minimized, but the reduction in variance never exceeded 2%. Furthermore, the empirically determined functions of the invariants did not appear to have recognizable structure and contained many oscillations. This type of behavior is often an indication that the algorithm has only found a local minimum in field of noise.

The results of the projection pursuit regression are consistent with the results presented in the previous section where the dependence on a single invariant was investigated. In both cases, the coefficients do appear to depend on the invariants, but that dependence is extremely weak. Accounting for this weak dependence on the invariants does not significantly reduce the coefficient spatial variation and thus is probably not worth pursuing further. More importantly, the large coefficient variation does not appear to be related to neglected dependence on the invariants, but rather to a weakness in the assumption that the subgrid-scale stress is solely a function of the velocity gradient.

2.5 Analysis for constant coefficients

In this section, we explore the accuracy of Eq. (11) when the coefficients are assumed to be constant in space. The constants are again determined through a least-squares procedure, this time minimizing the global error rather than the local error. The derivation of the global least-squares procedure is identical to that outlined in section 2.3, with the exception that the error is averaged over the domain

before it is differentiated with respect to the C_i. The end result is an expression analogous to Eq. (12):

$$C_i = < \mathrm{tr}(\mathbf{m}_i \mathbf{m}_j) >^{-1} < \mathrm{tr}(\mathbf{m}_j \boldsymbol{\tau}) >, \tag{21}$$

where <> indicates a spatial average. It is important to note that when the coefficients are determined globally, there will be non-zero error even when all five terms in Eq. (11) are used.

2.5.1 Results

As in section 2.3.1, all possible combinations of the various terms in Eq. (11) were tested. The correlation coefficients for the best and worst combinations of terms are shown in Figure 6. The actual terms corresponding to these groupings are listed in Table 2.

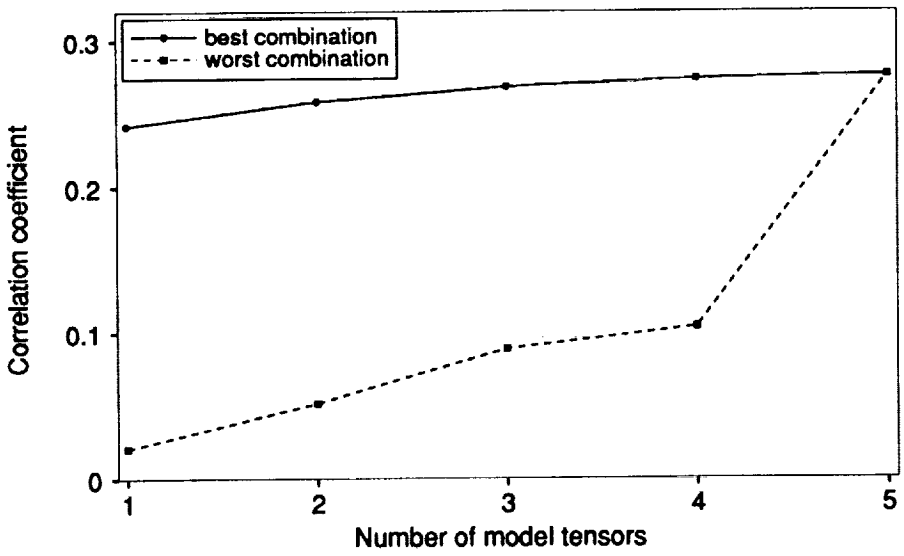

FIGURE 6. Correlation coefficients for the best and worst subsets of the terms in Eq. (11) - constant coefficients.

The best single term is again term 1, the Smagorinsky model. The correlation coefficient of the optimal groups increases as more terms are added, but the improvement is rather slight (15% increase from 1 to 5 terms). The optimal correlation coefficients also are rather low, never exceeding 0.28. In light of the slow increase with additional model terms, it appears that terms 2 through 5 are not nearly as important as the Smagorinsky model. This conclusion can also be drawn from the results for the worst groupings. The correlation coefficients for the worst groupings are far inferior to those of the best groupings, even when 4 terms are used. The Smagorinsky model is the last one to be added to the worst groupings, and the

Number of terms	Best combination	Worst combination
1	1	2
2	1, 2	2, 3
3	1, 2, 5	2, 3, 4
4	1, 2, 4, 5	2, 3, 4, 5
5	1, 2, 3, 4, 5	1, 2, 3, 4, 5

TABLE 2. Best and worst subsets of the model terms in Eq. (11) - constant coefficients.

correlation coefficient is seen to more double when this term is added (transition from 4 to 5 terms).

It is interesting to compare the results for variable and fixed coefficients (Figures 2 and 6). Several differences are readily apparent. The level of correlation is much lower in the case of fixed coefficients; if only a single term is used, the correlation coefficient for a constant coefficient is about one half the value obtained with a variable coefficient. As more terms are added, the correlation improves steadily when the coefficients are variable, but improves little if the coefficients are constant. In the variable coefficient case, there is little to choose between the best and worst groupings, whereas in the constant coefficient case, the differences are substantial. Overall, the variable coefficient results are much better than those for fixed coefficients.

The differences between the variable coefficient and constant coefficient results are due to differences in the scope of the minimization in the least-squares formulation. When the coefficients are allowed to vary in space, the error is minimized at each mesh point. This local minimization yields MN^3 degrees of freedom, where M is the number of model terms used and N^3 is the number of mesh points. When the coefficients are fixed in space, the error is minimized globally, and only M degrees of freedom are available. Evidently, the extra degrees of freedom are well utilized in the variable coefficient case, and superior correlations are obtained. At the same time, the additional degrees of freedom result in coefficients that vary greatly in space (recall Figure 3). This spatial dependence would be unknown in an actual LES, and thus the results of Figure 2 could not be realized in practice. The negative impact of the large coefficient variation is accounted for in Figure 6, and these results could be expected in practice.

The large coefficient variation also has an important physical implication. If it were true that the subgrid-scale stress depended *only* on the velocity gradient tensor, then the expansion given in Eq. (11) would be complete. The coefficients could vary in space, but this variance would have to result from dependence on the invariants listed in Eq. (11). Since the coefficients are observed to vary and this

variation does not appear to be connected with the invariants, it must be true that the subgrid-scale stress at one point in space depends on more than the velocity gradient at the same point. While this conclusion might have been anticipated, the more relevant issue is to what extent the expansion in Eq. (11) captures the dependence of the subgrid-scale stresses on the resolved variables. In view of Figure 6 and Table 2, it is clear that the dominant term is the Smagorinsky model. The remaining terms in Eq. (11) appear to be of lesser importance. In fact, if all of the terms are used, the correlation is only 15% higher than with the Smagorinsky model. Thus, at least for homogeneous isotropic flow, the expansion in Eq. (11) does not seem to contain much of the physical mechanisms by which the large scales influence the small scales.

2.6 Summary

A tensor relationship between subgrid-scale stress and the velocity gradient tensor has been developed. This relationship takes the form of a series expansion involving products of the strain and rotation rate tensors. The expansion was used as a modeling hypothesis, and the latter was evaluated using direct numerical simulation data for homogeneous isotropic turbulence. The Smagorinsky model, which is one of the terms in the expansion, was found to be the dominant term. The remaining terms were found to be of lesser importance and, when included, did not significantly improve upon the Smagorinsky model. These results suggest that while the expansion is exact, the inherent assumption that the subgrid-scale stress depends only on the velocity gradient tensor is not well supported by the numerical simulation data for homogeneous isotropic turbulence at low Reynolds number.

3. Future plans

The conclusions drawn in the previous section apply only to homogeneous isotropic turbulence at low Reynolds number. Both the success of the model and the coefficient values could be Reynolds number dependent. This issue will be addressed by repeating the tests with higher Reynolds number DNS data. For this purpose, forced homogeneous isotropic simulation data is available with Reynolds number roughly four times greater than that used in the present study. In addition to Reynolds number effects, the success of the proposed model may be related to the flow situation. For example, it is quite possible that the model would work better in a shear flow where the effects of rotation are more pronounced. This possibility will be explored by testing the model with DNS data for homogeneous turbulent shear flow and for turbulent channel flow. If these results are sufficiently encouraging, the model will be used in an actual large eddy simulation and the results compared with experimental or DNS data. For the purpose of simulation, the procedure of §2.5 will be used to assign constant values to the expansion coefficients.

A separate attempt will be made to use the model in conjunction with the dynamic procedure of Ghosal *et al.*(this volume). In this procedure, information contained in the resolved field will be used to estimate the value of the expansion coefficients as a function of space and time. This approach has the potential to recover the accuracy displayed in Figure 2 since the coefficients will be free do develop

any arbitrary degree of variability.

Acknowledgements

In addition to support from the Center for Turbulence Research, this work was supported in part by the Air Force Office of Scientific Research, the Office of Naval Research, and the Department of Energy. TSL acknowledges support from the ONR under grant N00014-91-J-4072 and from the AFOSR under grant F49620-92-J-0003. EAN acknowledges support from the CTR, ONR and DOE.

REFERENCES

CLARK, R. A., FERZIGER, J. H., & REYNOLDS, W. C. 1979 Evaluation of subgrid-scale models using an accurately simulated turbulent flow. *J. Fluid Mech.* **91**, 1-16.

COMTE-BELLOT, G., & CORRSIN, S. 1971 Simple Eulerian time correlation of full and narrow-band velocity signals in grid-generated 'isotropic' turbulence. *J Fluid Mech.* **48**, 273-337.

FRIEDMAN J. H. & STUETZLE W. 1981 Projection pursuit regression. *J. Amer. Stat. Assoc.* **76**, 817

MENEVEAU, C. LUND, T. S., & MOIN, P. 1992 Search for subgrid-scale parameterization by projection pursuit regression. *Proceedings of the 1992 summer program*, CTR, Stanford Univ, 61-80.

MCMILLAN O. J. & FERZIGER J. H 1979 Direct testing of subgrid-scale models. *AIAA J.* **17**, 1340

PIPES, L. A. & HOVANESSIAN, A. 1969 *Matrix-computer methods in engineering*, J. Wiley & Sons.

PIOMELLI U., MOIN P. & FERZIGER J.H. 1988 Model consistency in large eddy simulation of turbulent channel flows. *Phys. Fluids.* **31**, 1884

POPE, S. B. 1975 A more general effective-viscosity hypothesis. *J. Fluid Mech.* **72**, 331-340.

RIVLIN, R. S. & ERICKSEN, J. L. 1955 Stress-deformation rates for isotropic materials. *Journal of Rational Mechanics and Analysis.* **4**, 323-425.

ROGALLO R. 1981 Numerical experiments in homogeneous turbulence. *NASA Tech. Mem.*, 81315.

SPENCER, A. J. M & RIVLIN, R. S. 1959 The theory of matrix polynomials and its application to the mechanics of isotropic continua. *Archive for Rational Mechanics and Analysis.* **2**, 309-336.

SMAGORINSKY, J. 1963 General circulation experiments with the primitive equations. *Mon. Weather Rev.* **91**, 99-164.

TENNEKES, H. & LUMLEY, J. L. 1972 *A first course in turbulence*, MIT Press.